International Journal of Heat and Mass Transfer 127 (2018) 1025–1039

Contents lists available at ScienceDirect

International Journal of Heat and Mass Transfer

journal homepage: www.elsevier.com/locate/ijhmt

An entransy based method for thermal analysis and management of high heat density data centers

Hao Tian [a], Hang Liang [b,*], Zhen Li [c]

[a] Changchun Institute of Optics, Fine Mechanics and Physics, Chinese Academy of Sciences, Changchun 130033, China
[b] Jilin University, Changchun 130021, China
[c] Tsinghua University, Beijing 100000, China

ARTICLE INFO

Article history:
Received 5 April 2018
Received in revised form 3 June 2018
Accepted 7 July 2018
Available online 2 August 2018

0. Introduction

With the fast development of new IT techniques (e.g. cloud service, AI, mobile internet), the past few years have witnessed a sharp increasing demand for massive data storage, computing and processing. A large number of data centers have been built and updated in consequence, resulting in a dramatic rise of power demand. During the past 10 years, the peak pay load of rack level has been increased from less than 10 kW to over 30 kW in average [1]. Meanwhile, due to the widely use of highly integrated chips (such as CPU and GPU), the peak heat flux of IT equipment also showed a steep rise to nearly 50 W/cm^2 [2], which has been commonly seen in high performance commercial blade servers. With increasingly higher heat flux and more compact layout, hot spot is no longer a locally over-heating phenomena, but a fetal threat to the thermal health of entire data center [3,4]. Consequently, over 40% of annual operating cost has been spent on air-conditioning [5] and this ratio is expected to exceed 60% in next five years [5]. Now that thermal management significantly affects the operational security and cost of data centers, to find a more effective solution with better energy performance becomes a key issue for thermal management of future high heat density data centers [6–8].

Data center thermal management aims to maintain facility temperature and energy cost within a reasonable range, through the adjustment and optimization of IT payload, facility layout, air flow pattern, operating mode and cooling configuration. Traditionally, the fundamental theory of data center thermal analysis contains heat transfer rules and thermodynamic laws only [9–12]. Based on which, various numerical and experimental models have been developed to predict energy flow and temperature distribution inside data centers, from chip level to room space [13–20]. In state of the art, most of the models are based on *Navier-Stokes* equation for flow computing, coupled with continuity and heat transfer equations, with different boundary and initial conditions [21–23]. Other models use new evaluating indicator (*SHI*, *RHI*, *RCI*), revised algorithm (POD, ROM, artificial network method) or advanced data processing tools to achieve faster calculation, better evaluation of the overall performance of data center thermal management, further optimization on operating parameters, or more accurate fitting of test data [24–26].

Besides of theoretical research, many case studies have been introduced in data center thermal design and management [27–30], some of which have succeed to offer guidance to improve cooling efficiency, reduce hot spot and energy cost with specified boundary and operating conditions.

Recently, as more urgent needs for cooling energy benefits emerged, analysis on the availability of outdoor free cooling potential and maximum energy efficiency becomes focused issues. Consequently, much attention has been paid to thermodynamic based theories. As typical examples, exergy theory has been widely used to optimize thermal management and improve data center energy performance [31–33]. Exergy method gives revised air flow pattern, power plant and payload allocation in data centers, maximizes the potential of useful work, based on the principle of least exergy loss/entropy generation.

1. Entransy theory

1.1. Entransy theory introduction

Recent years, Guo et al. [34–41] proposed a new physical quantity called entransy, to represent heat transport potential, by analogy with electric and gravity field. In electric filed, with the same potential difference, the more quantity of electricity a body carried,

* Corresponding author.
E-mail addresses: tianh@ciomp.ac.cn (H. Tian), jellolh@sina.com (H. Liang).

https://doi.org/10.1016/j.ijheatmasstransfer.2018.07.036

the more field work occurs, resulting in more loss of potential energy. By analogy, in temperature field, the heat flux q driven by temperature difference δT always causes an irreversible dissipation, representing a kind of potential energy loss. In temperature field, such loss can be quantified as $\Delta J = q \times \delta T$. ΔJ is defined as entransy dissipation, which represents the irreversible loss of heat transport ability. Furthermore, this definition means that, in temperature field, the entransy J can be represented by heat flux q at temperature T as $J = q \times T$. Thus, the entransy dissipation ΔJ during a heat transport process, from initial (q_1, T_1) to final (q_2, T_2), can be quantified as $\Delta J = q_1 \times T_1 - q_2 \times T_2$.

For continuous process in temperature field

$$\Delta J = \int_{T_1}^{T_2} q(T)dT \tag{1-1}$$

Eq. (1-1) offers a new graphical expression for entransy flow and dissipation, called *T-Q* chart. Fig. 1 is a *T-Q* chart representing a steady state open system with heat transport process inside, with a heat/cold source of constant temperature T_h/T_c. Two fluids are involved, with the inlet and outlet temperature of T_{in}/T_o and T_c/T_l respectively.

For heat transfer process from heat source (T_h) to fluid (T_{in}/T_o), according to Eq. (1-1), the corresponding entransy dissipation ΔJ_h is

$$\Delta J_h = \int_{T_{in}}^{T_o}(T_h - T)dq = \int_{T_{in}}^{T_o}(T_h - T)(cmdT)$$
$$= cm(T_o - T_{in})\left[T_h - \frac{1}{2}(T_o + T_{in})\right] = q\Delta T_{mean} \tag{1-2}$$

In Eq. (1-2), cm represents mass and heat capacity flow rate of the fluid, W/K; q is the total heat removed, W; ΔT_{mean} refers to the mean temperature difference between heat source and fluid, K. ΔJ_h is graphically illustrated by the yellow region in *T-Q* chart in Fig. 1.

For heat transfer process between two fluids, in which one fluid is cooled from T_o to T_{in}, while the other is heated from T_c to T_l, according to Eq. (1-1), the corresponding entransy dissipation ΔJ_l is (see Fig. 2)

$$\Delta J_l = \int_{T_{in}-T_c}^{T_o-T_l} \Delta T dq = \int_{T_{in}-T_c}^{T_o-T_l} \Delta T d(KF\Delta T)$$
$$= \frac{1}{2}KF[(T_o - T_l)^2 - (T_{in} - T_c)^2] \tag{1-3}$$

The total transported heat q can be expressed as

$$q = \int dq = \int_{T_{in}-T_c}^{T_o-T_l} KFd(\Delta T) = KF[(T_o - T_l) - (T_{in} - T_c)] \tag{1-4}$$

Bring Eq. (1-4) back to Eq. (1-3), the entransy dissipation ΔJ_l is finally obtained as

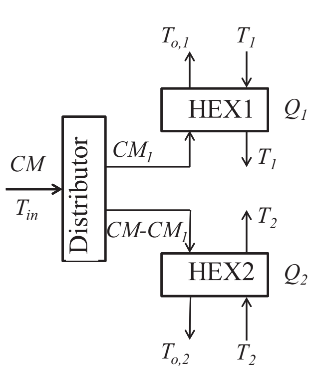

Fig. 1. Solo heat transfer process for verification.

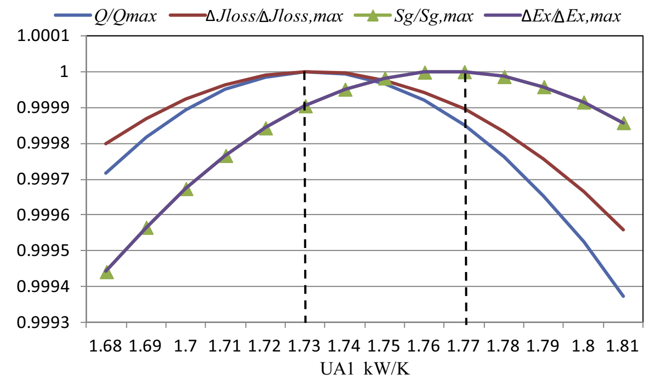

Fig. 2. Variation of transported heat, exergy loss, entropy generation and entransy dissipation with increment of heat transfer ability UA_1.

$$\Delta J_l = q\frac{1}{2}[(T_o - T_l) + (T_{in} - T_c)] = q\Delta T_{mean} \tag{1-5}$$

In Eqs. (1.3)-(1.5), *KF* represents heat transfer ability for each integrating unit, W/K, which is assumed to be constant during heat transport. ΔT is the temperature difference of two fluids for each integrating unit, K. ΔJ_l is illustrated by the green region in *T-Q* chart in Fig. 1.

Using the same derivation as Eq. (1-2), the entransy dissipation between the fluid and cold source ΔJ_c can be rewritten as

$$\Delta J_c = \int_{T_c}^{T_l}(T - T_c)(cmdT) = cm\int_{T_c}^{T_l} TdT - cmT_c\int_{T_c}^{T_l} dT$$
$$= cm(T_l - T_c)\left[\frac{1}{2}(T_l + T_c) - T_c\right] = \frac{1}{2}q(T_l - T_c) \tag{1-6}$$

ΔJ_c expressed by Eq. (1-6) is represented by the blue region in *T-Q* chart in Fig. 3.

Bring Eqs. (1.2), (1.5) and (1.6) into Eq. (1-7) to get the total entransy dissipation ΔJ as represented by Eq. (1-8).

$$\Delta J = \Delta J_h + \Delta J_l + \Delta J_c \tag{1-7}$$

$$\Delta J = q\left[T_h - \frac{1}{2}(T_o + T_{in})\right] + q\frac{1}{2}[(T_o - T_l) + (T_{in} - T_c)]$$
$$+ \frac{1}{2}q(T_l - T_c) = q(T_h - T_c) \tag{1-8}$$

Eq. (1-8) reveals the behavior characteristics of entransy flow and dissipation for a steady state open system, with at least two fluids involved.

With Eq. (1-8) and *T-Q* chart, entransy theory turns a complex heat transfer system into a simple mathematical field model, with all thermal behavior quantified by entransy flow and dissipation.

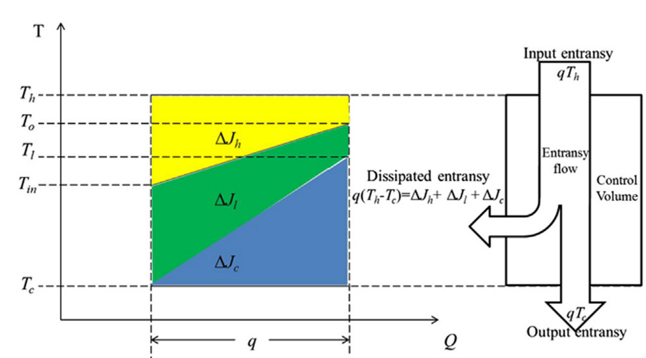

Fig. 3. T-Q chart of entransy flow and dissipation.

Thus, a new feasible solution for multi-scale data center thermal management becomes possible, as long as all the typical thermal behavior for each level is turned into the mathematical model of entransy flow and entransy dissipation.

1.2. The suitability of entransy theory to heat transfer analysis

Fundamentally, entropy/exergy theory along with the second law of thermodynamics applies to thermo-power process, which contains the conversion of heat into power. As to solo heat transport process without any heat-power conversion, such as heat transport between fluids through heat exchangers, Chen [42] has proved both the suitability and advantage of entransy theory over entropy/exergy theory, using a case study of fluid heat exchanging optimization to compare the heat transfer performance between entransy/entropy/exergy theory, Li and Tian [43] has attempted to use entransy dissipation theory to analyze and optimize data center heat transfer process.

Although former studies have proved the applicability of entransy dissipation method to the thermal analysis and optimization of heat transfer/exchange process, including in data centers. However, a complete model based on entransy dissipation analysis for multi-level heat transfer process in data centers has not been built yet. Consequently, so far the entransy based methods or principles which can guide the improvement or offer better measures for data center thermal management is still in lack, especially for the quantitative analysis on undesired air mixing, which significantly impacts both the thermal and energy performance of data centers. This is one of the core subjects of our work in this paper.

2. Entransy dissipation model for multi-level heat transfer process in data centers

2.1. Entransy analysis model of CPU level heat transfer

The heat transfer process between CPU and cooling fluid (air, water, refrigerants, and so on) can be modeled as a heat source with constant temperature T_{cpu}, and a cycle fluid with inlet/exhaust temperature of T_{in}/T_o, as demonstrated by Fig. 4.

The heat flux and average temperature of CPU is assumed to be constant and represented by Q_{cpu} and T_{cpu}, respectively. The entransy dissipation of CPU cooling process equals to the area of yellow region in *T-Q* chart in Fig. 1, which can be calculated as

$$\Delta J_{cpu} = \frac{1}{2}Q_{cpu}[(T_{cpu} - T_{in}) + (T_{cpu} - T_o)] = Q_{cpu}\left[T_{cpu} - \frac{1}{2}(T_{in} + T_o)\right] \tag{2-1}$$

2.2. Entransy analysis model of rack level heat transfer

As to rack level heat transfer, the undesired air mixing is a major problem, which increases CPU inlet air temperature, disturbs cooling distribution or even causes hot spot, demonstrated by Fig. 5.

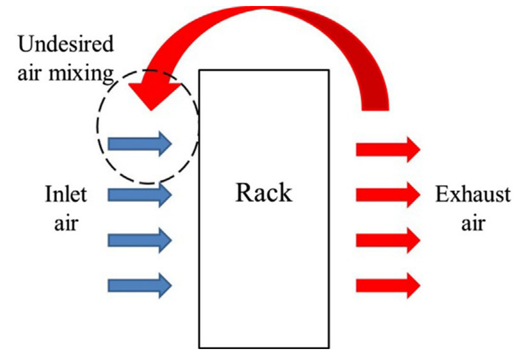

Fig. 5. Undesired air mixing in rack level.

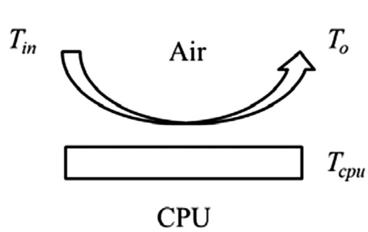

Fig. 4. CPU model with air cooling.

Therefore, thermal behavior of rack level is more complex than CPU level. To quantify the effect of undesired air mixing, entransy model must be built. To calculate entransy dissipation of multi-air mixing, the fundamental expression of two air streams mixing should first be derived.

For steady convective heat transfer process with constant thermal properties and no internal heat source, the energy equation is

$$\nabla \cdot (k\nabla T) = \rho c_p \vec{V} \cdot \nabla T \tag{2-2}$$

k represents thermal conductivity, W/(m K); ρ represents density, kg/m^3; c_p represents specific heat, kJ/(kg K); $\vec{V}$ represents velocity vector, m/s; T represents thermal temperature, K. Left side of Eq. (2-2) represents diffusion term caused by heat conduct, and right side of Eq. (2-2) represents convection term caused by fluid flow.

Multiply both sides of Eq. (2-2) by thermal temperature T to get Eq. (2-3)

$$T\nabla \cdot (k\nabla T) = \rho c_p T\vec{V} \cdot \nabla T \tag{2-3}$$

Perform deformation on the right side of Eq. (2-1) using vector operation rule to get Eq. (2-4)

$$\rho c_p \vec{V}T \cdot \nabla T = \frac{1}{2}\rho c_p \vec{V} \cdot \nabla T^2 = \frac{1}{2}\rho c_p[\nabla \cdot (\vec{V}T^2) - T^2\nabla \cdot \vec{V}] \tag{2-4}$$

Put mass conservation equation (continuity equation) $\nabla \cdot \vec{V} = 0$ into Eq. (2-4) to get Eq. (2-5)

$$\rho c_p \vec{V}T \cdot \nabla T = \nabla \cdot \left(\frac{1}{2}\rho c_p \vec{V}T^2\right) \tag{2-5}$$

Perform deformation on the left side of Eq. (2-1) using vector operation rule to get Eq. (2-6)

$$T\nabla \cdot (k\nabla T) = \nabla \cdot (Tk\nabla T) - k(\nabla T)^2 \tag{2-6}$$

Put Eqs. (2-5) and (2-6) back into Eq. (2-2) to get Eq. (2-7)

$$\nabla \cdot \left(\frac{1}{2}\rho c\vec{V}T^2\right) = \nabla \cdot (Tk\nabla T) - k(\nabla T)^2 \tag{2-7}$$

Define convective entransy flow $\vec{J}_v$ (unit: W K/m^2) and conductive entransy flow $\vec{J}_t$ (unit: W K/m^2) as follows

$$\vec{J}_v = \frac{1}{2}\rho c_p \vec{V}T^2 \tag{2-8}$$

$$\vec{J}_t = T\vec{q}_t = -Tk\nabla T \tag{2-9}$$

Put Eqs. (2-8) and (2-9) back into Eq. (2-7) to get Eq. (2-10)

$$\nabla \cdot \vec{J}_v + \nabla \cdot \vec{J}_t = -k(\nabla T)^2 \tag{2-10}$$

Terms on left side of Eq. (2-10) $\nabla \cdot \vec{J}_v$, $\nabla \cdot \vec{J}_t$ represent the variation of convective entransy flow $\vec{J}_v$ (unit: W K/m^3) and conductive entransy flow $\vec{J}_t$ (unit: W K/m^3) carried by fluid respectively. Term on right side of Eq. (2-10) $-k(\nabla T)^2$ represents the quantity of entransy flow lost inside unit volume caused by fluids temperature discrepency (unit: W K/m^3), representing heat transfer ability loss caused by irreversiblities. Eq. (2-10) is the differential form of entransy conservation equation for convective heat transfer process with steady state, constant thermal properties and no internal heat source.

Integrate Eq. (2-10) in space control volume Ω, get the integral form of entransy conservation equation for convective heat transfer in finite space volume as Eq. (2-11)

$$\int_\Omega (\nabla \cdot \vec{J}_v) d\Omega + \int_\Omega (\nabla \cdot \vec{J}_t) d\Omega = \int_\Omega (-k(\nabla T)^2) d\Omega \tag{2-11}$$

Perform deformation on left terms of Eq. (2-11) using Gauss Theorem, convert volume integral into surface integral to get Eq. (2-12)

$$\oint_S \vec{J}_v \cdot d\vec{S} + \oint_S \vec{J}_t \cdot d\vec{S} = \oint_S \vec{J}_v \cdot \vec{n} dS + \oint_S \vec{J}_t \cdot \vec{n} dS = \int_\Omega (-k(\nabla T)^2) d\Omega \tag{2-12}$$

Eq. (2-12) is the differential form of entransy conservation equation for convective heat transfer process on the surface of finite space control volume, $\vec{n}$ is the normal vector of surface dS which surrounds the control volume Ω. For cubic control volume shown by Fig. 6, all surface normal vectors are parallel to axis of X, Y, Z directions. In this case, Eq. (2-12) can be represented by cartesian coordinates as Eq. (2-13)

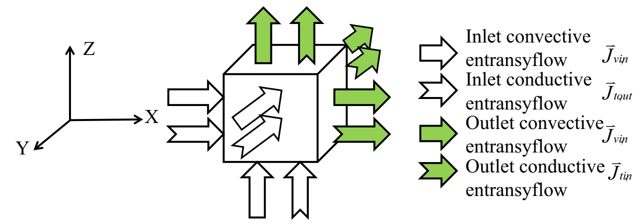

Fig. 7. Entransy flow into and out of space control volume.

For cubic space control volume shown by Fig. 7, term $\oint_S \vec{J}_v \cdot dS$ on the left side of Eq. (2-13) represents total flux of convective entransy flow $\vec{J}_v$ through closed surface S, which is the net convective entransy flow into and out of this control volume. Term $\oint_S \vec{J}_t \cdot dS$ on the left side of Eq. (2-13) represents total flux of conductive entransy flow $\vec{J}_t$ through closed surface S, which is the net conductive entransy flow into and out of this control volume. Term $-k\int_\Omega (\nabla T)^2 d\Omega$ on the right side of Eq. (2-13) represents the difference of net entransy flow through closed surface S, which equals to the entransy dissipation of the convective heat transfer process in this control volume.

Eq. (2-13) indicates that, for heat transfer process in an open thermal system, fluid that flows into and out of the system complies with energy conservation but has heat transfer ability loss due to the temperature discrepancy. The time needed for fully mixing determines how fast heat transfer ability is being lost during the mixing, which is mainly dependent on heat conductivity k. However, the final temperature of fully mixed fluids and the mixing entransy dissipation are not decided by k only. The temperature gradient along specific direction also effects the mixing entransy dissipation significantly, which means airflow organization is a feasible approach to minimize the undesired mixing loss.

$$\begin{aligned}
&\frac{1}{2}\rho c v\Big[\Big(V_{x,in}\Delta Y \Delta Z T_{x,in}^2 + V_{y,in}\Delta X \Delta Z T_{y,in}^2 + V_{z,in}\Delta X \Delta Y T_{z,in}^2\Big) - \Big(V_{x,out}\Delta Y \Delta Z T_{x,out}^2 + V_{y,out}\Delta X \Delta Z T_{y,out}^2 + V_{z,out}\Delta X \Delta Y T_{z,out}^2\Big)\Big] \\
&- k\left[\left(T_{x,in}\Delta Y \Delta Z\left(\frac{\partial T}{\partial X}\right)_{in} + T_{y,in}\Delta X \Delta Z\left(\frac{\partial T}{\partial Y}\right)_{in} + T_{z,in}\Delta X \Delta Y\left(\frac{\partial T}{\partial Z}\right)_{in}\right) - \left(T_{x,out}\Delta Y \Delta Z\left(\frac{\partial T}{\partial X}\right)_{out} + T_{y,out}\Delta X \Delta Z\left(\frac{\partial T}{\partial Y}\right)_{out} + T_{z,out}\Delta X \Delta Y\left(\frac{\partial T}{\partial Z}\right)_{out}\right)\right] \\
&= k\int_\Omega \left(\left(\frac{\partial T}{\partial X}\right)^2 + \left(\frac{\partial T}{\partial y}\right)^2 + \left(\frac{\partial T}{\partial Z}\right)^2\right) d\Omega
\end{aligned} \tag{2-13}$$

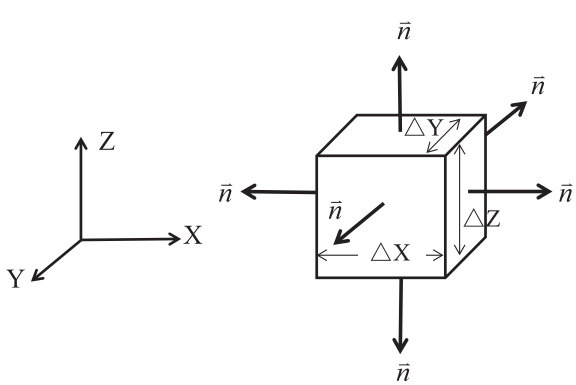

Fig. 6. Cubic control volume in data center space.

2.3. Entransy model analysis of room level heat transfer

For a given data center with p CRAC units, n racks and m CPUs inside each rack, based on Eqs. (1-7), (1-8), the entransy dissipation in terms of CPU level cooling, rack level air mixing and CRAC level heat removal are related as Eq. (2-14), in which J_{in} and J_{out} represents the input and output entransy flow, respectively.

$$\Delta J_{loss,room} = J_{in} - J_{out} = \Delta J_{cpu} + \Delta J_{mixing} + \Delta J_{crac} \tag{2-14}$$

The input entransy flow J_{in} into the data center is calculated by each individual heat source (CPU) temperature $T_{cpu,i}$ and dissipated heat $Q_{cpu,i}$ inside all racks, as expressed by Eq. (2-15).

$$J_{in} = \sum_{i=1}^{n \times m} Q_{cpu,i} T_{cpu,i} \tag{2-15}$$

The output entransy flow J_{out} out of the data center can be calculated by each individual cold source (CRAC units) temperature $T_{crac,j}$ and dissipated heat $Q_{crac,j}$ inside the data center room, as expressed by Eq. (2-16).

$$J_{out} = \sum_{j=1}^{p} Q_{crac,j} T_{crac,j} \tag{2-16}$$

With energy conservation as

$$\sum_{i=1}^{n\times m} Q_{cpu,i} = \sum_{j=1}^{p} Q_{crac,j} \tag{2-17}$$

When fluid thermal parameter (tempertaure, mass flowrate) is considered, a more widely used entransy model can be built for rack level air mixing and CRAC heat removal as follows.

Rack can be modeled as a steady state open thermal system with n CPUs, inlet and outlet airflows. Assuming the temperature and mass flowrate for each inlet/outlet airflow is represented by $T_{a,in,i}/T_{a,o,i}$, $CM_{a,in,i}/CM_{a,o,i}$, respectively, and air mixing takes place randomly among n CPUs. According to Eq. (2-13), rack level air mixing entransy dissipation ΔJ_{mixing} can be deduced as follows

$$\begin{aligned}\Delta J_{mixing} &= J_{air,in,rack} - J_{air,out,rack} \\ &= \sum_{i=1}^{n}\left(\frac{1}{2}CM_{a,in,i}T_{a,in,i}^2 + Q_{cpu,i}T_{cpu,i} - \frac{1}{2}CM_{a,o,i}T_{a,o,i}^2\right)\end{aligned} \tag{2-18}$$

CRAC can be modeled as a steady open thermal system with a refrigerant coil (cold source), one in-flow (room return air) and one outflow (CRAC supply air). Assuming the temperature and mass flowrate for inlet/outlet airflow is represented by $T_{a,in,j}/T_{a,o,j}$, $CM_{a,in,j}/CM_{a,o,j}$, respectively, refrigerant coil temperature is represented by $T_{crac,j}$, and no air mixing occurs in CRAC units. According to Eq. (2-13), the entransy dissipation of air-coil heat exchanging process (room terminal heat removal) ΔJ_{crac} can be deduced as follows

$$\begin{aligned}\Delta J_{crac} &= \sum_{j}(J_{air,in,crac} - J_{air,out,crac}) \\ &= \sum_{j=1}^{p}\left(\frac{1}{2}CM_{a,in,j}T_{a,in,j}^2 - Q_{crac,j}T_{crac,j} - \frac{1}{2}CM_{a,o,j}T_{a,o,j}^2\right)\end{aligned} \tag{2-19}$$

Put Eqs. (2.15)-(2.19) back into Eq. (2-14), the room level entransy dissipation model for a given data center can be expressed as follows

$$\begin{aligned}\Delta J_{loss,room} &= \sum_{i=1}^{n\times m} Q_{cpu,i}T_{cpu,i} - \sum_{j=1}^{p} Q_{crac,j}T_{crac,j} \\ &\quad - \sum_{i=1}^{n}\left(\frac{1}{2}CM_{a,in,i}T_{a,in,i}^2 + Q_{cpu,i}T_{cpu,i} - \frac{1}{2}CM_{a,o,i}T_{a,o,i}^2\right) \\ &\quad - \sum_{j=1}^{p}\left(\frac{1}{2}CM_{a,in,j}T_{a,in,j}^2 - Q_{crac,j}T_{crac,j} - \frac{1}{2}CM_{a,o,j}T_{a,o,j}^2\right) \\ &= \sum_{i=1}^{n}\left(\frac{1}{2}CM_{a,in,i}T_{a,o,i}^2 - \frac{1}{2}CM_{a,o,i}T_{a,in,i}^2\right) \\ &\quad + \sum_{j=1}^{p}\left(\frac{1}{2}CM_{a,in,j}T_{a,o,j}^2 - \frac{1}{2}CM_{a,o,j}T_{a,in,j}^2\right) \\ &= \left(\sum_{i=1}^{n}\frac{1}{2}CM_{a,in,i}T_{a,o,i}^2 + \sum_{j=1}^{p}CM_{a,in,j}T_{a,o,j}^2\right) \\ &\quad - \left(\sum_{i=1}^{n}\frac{1}{2}CM_{a,o,i}T_{a,in,i}^2 + \sum_{j=1}^{p}\frac{1}{2}CM_{a,o,j}T_{a,in,j}^2\right) \\ &= J_{a,input} - J_{a,output}\end{aligned} \tag{2-20}$$

Eq. (2-20) tells that, for a given data center space with adiabatic envelops, entransy dissipated by mixing of different temperature airflows has nothing to do with properties of IT equipments or CRAC units, essentially, it is a heat transfer caused dissipation, determined by airflow pattern, air flowrate and temperature.

To better explain the entransy dissipation for room level in data centers, each dissipation occurs through the entransy flow path is illustrated by Fig. 8, corresponds to Eqs. (2.14)-(2.19).

Divide the total entransy dissipation value ΔJ_{loss} by total heat $Q = \sum_{i=1}^{n} Q_{cpu,i}$, to get the temperature penalty ΔT paid for the undesired air mixing

$$\Delta T = \frac{\Delta J_{loss}}{Q} = \frac{\Delta J_{loss}}{\sum_{i=1}^{n} Q_{cpu,i}} \tag{2-21}$$

All analysis above shows that, entransy dissipation caused by air mixing and heat transfer process in data center space can be modeled and calculated, which means, the heat transfer ability loss and thermal performance decrease in data centerscan be quantified. Characteristics of entransy dissipation caused by rack level air mixing offers a new approach to evaluate how airflow pattern influences data center thermal performance. Therefore,

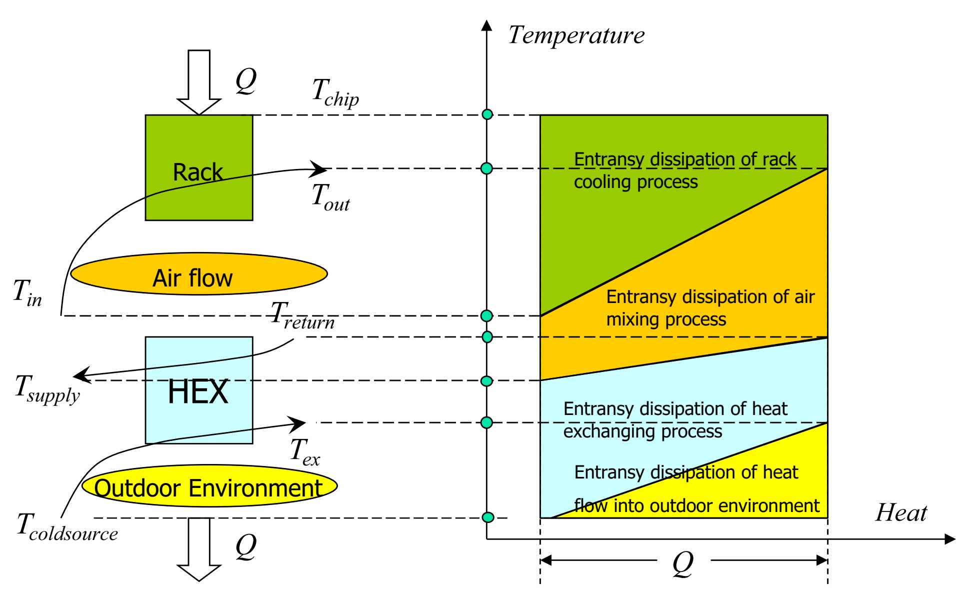

Fig. 8. Entransy dissipation along a typical heat transport path in data centers.

understanding the distribution and variation of air mixing entransy dissipation among data center space not only helps to reduce hot spots, evaluate airflow organization, improve the performance of data center thermal management, it also provides a new guideline for data center thermal management -least entransy dissipation principle, which has been proved to be more appropriate and effective in optimization of complex heat transfer system. A case study is performed to verify the entransy model.

3. Case study

3.1. Data center configuration

A CRAC retrofitting project of an operating data center in Beijing is performed, using entransy based theory. The basic configuration of the data center is listed in Table 1.

Fig. 9 shows the original layout and air flow pattern of the data center. Fig. 10 gives the pictures of former CRAC units and racks before retrofitting.

It can be seen from Fig. 9 that, the air-flow organization is rather poor. Supply air from No. 2 and No. 3 CRAC unit directly enters into the hot aisle of 24 racks. Such air flow pattern not only wastes the valuable cooling air, making certain racks cooling-starving, the consequently occurred air mixings by CRAC supply air and rack exhausted air worsen the entire thermal health of the data center space, and finally forms a vicious circle.

Table 1
Basic information of the retrofitting data center in Beijing.

Data center size	Envelope	Rack number	Rack power
20 m × 6 m × 3 m	One external wall	39	50–60 kW
CRAC number	Cooling capacity	Indoor temperature	Indoor humidity
3	80 kW	23–25 °C	40–65%

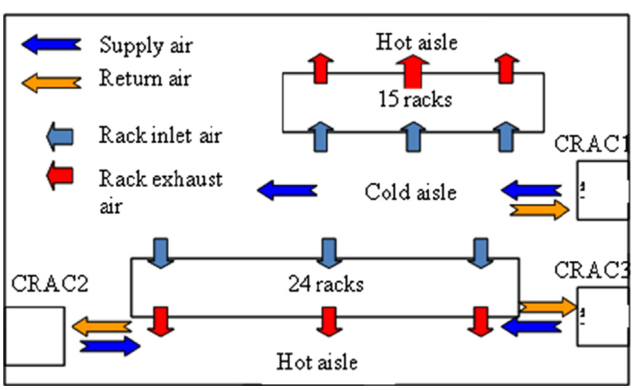

Fig. 9. Data center configuration.

3.2. Performance testing before retrofitting

Fig. 11 gives the testing data of inlet air temperature for all racks before retrofitting. It can be seen that for most racks (27 racks), the available cooling air temperature is actually higher than 25 °C, with only 2 racks enjoy cooling air less than 15 °C. Such non-uniform indoor thermal environment is mainly caused by poor air flow organization and undesired air mixing, which can be seen in the following test.

Fig. 12 shows the testing exhausted air temperature of 3 typical racks with different payload before retrofitting. A temperature difference as large as 7 K tells that, besides air-flow influence, the cooling starving racks (see Fig. 11) also contributes significantly to the non-uniform temperature distribution in data center space, by exhausting much hotter air than other racks.

Fig. 13 gives the testing supply air temperature of 3 CRAC units before retrofitting. A temperature difference of 6 K between No. 1 and No. 3 CRAC units indicates a severe mixing between return air and ambient air. The apparently fluctuated supply air temperature of No. 2 CRAC unit indicates a poor air-flow around, which turns out to easily cause severe air mixings and makes a worse indoor thermal environment in turn.

3.3. Retrofitting case

To effectively eliminate the defect of undesired air mixing above and improve the energy performance of this data center, both the method and systematic structure of thermal management needs retrofitting, based on deep entransy analysis. A feasible and fundamental approach is to perform a quantitative entransy dissipation comparison for several typical solutions of data center thermal management, and propose a optimum scheme with best entransy performance.

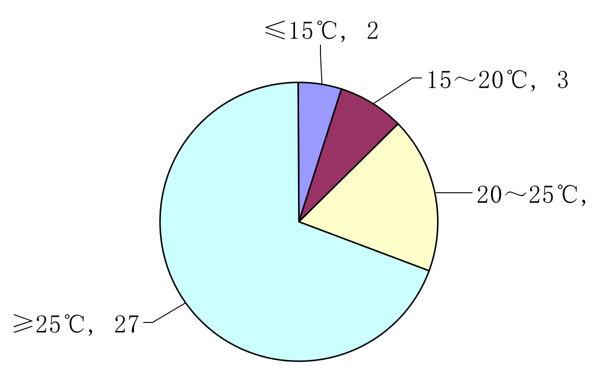

Fig. 11. Rack inlet air temperature before retrofitting.

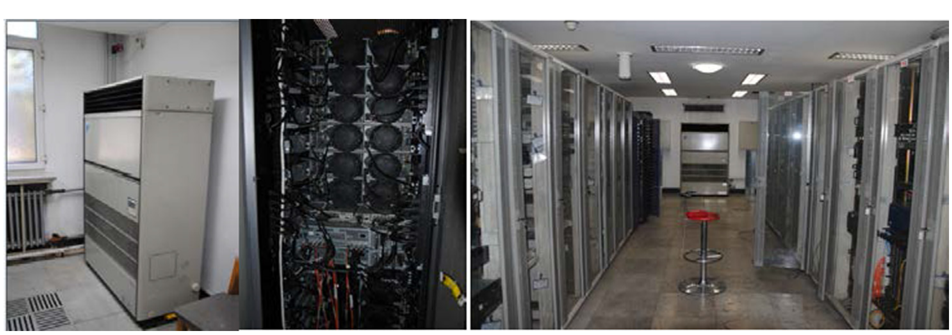

Fig. 10. Former CRAC units and racks before retrofitting.

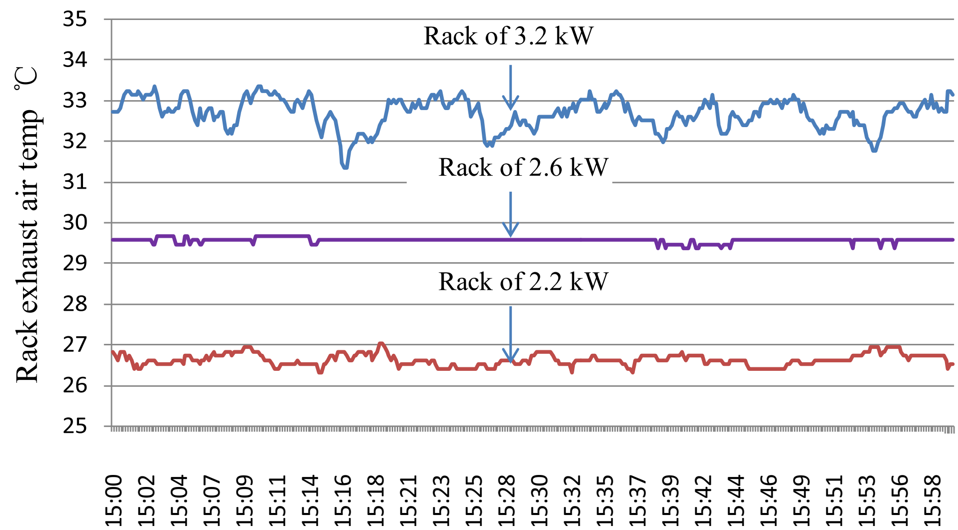

Fig. 12. Rack exhausted air temperature before retrofitting.

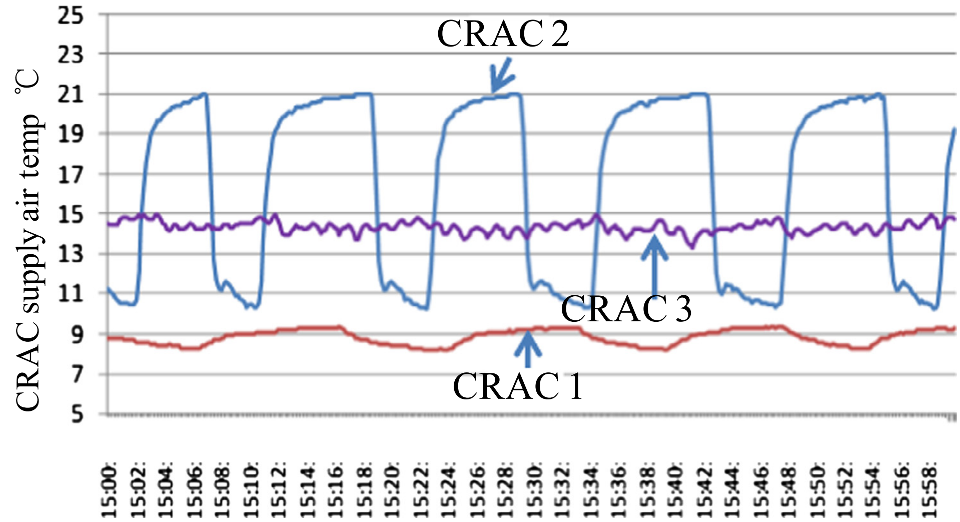

Fig. 13. CRAC supply air temperature before retrofitting.

3.3.1. Entransy dissipation analysis

Fig. 14a illustrates a simplified liquid cooling solution of data centers, which directly removes heat from servers by liquid media (water, refrigerant) loop and transports the heat to chilled water loop, which finally transfers the heat to CRAC units. The whole heat transport path is extremely compact with no air involved.

Fig. 14b illustrates an ideal air cooling configuration without hot/cold air mixings. All exhaust hot air from servers is collected and delivered to the water-side terminals near the servers, and exchanges heat with the chilled water in that terminal. The air flow circle and heat exchanging process is completely sealed inside the rack. The heat is then transported by chilled water loop to CRAC units. Such configuration is very compact to reduce the chance of hot air escaping and mixing with ambient cooling air around the racks.

Fig. 14c shows a typical air cooling scenario in data centers, where undesired air mixing occurs, with rack exhaust hot air circulated into cold aisles and cooling air direct short circuit into CRAC unit.

Fig. 14d shows a optimum air cooling solution with no undesired mixings, in which the air circle goes through a multi-step

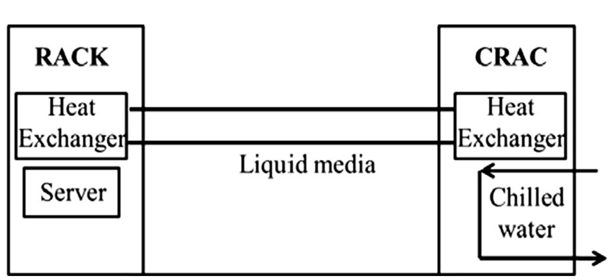

Fig. 14a. Liquid cooling solution.

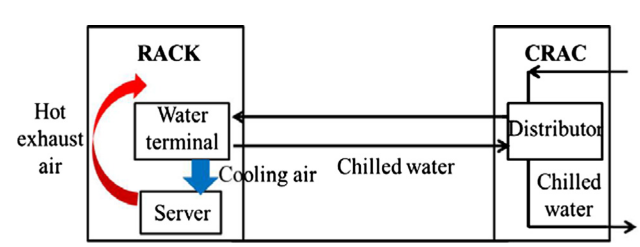

Fig. 14b. Ideal air cooling solution.

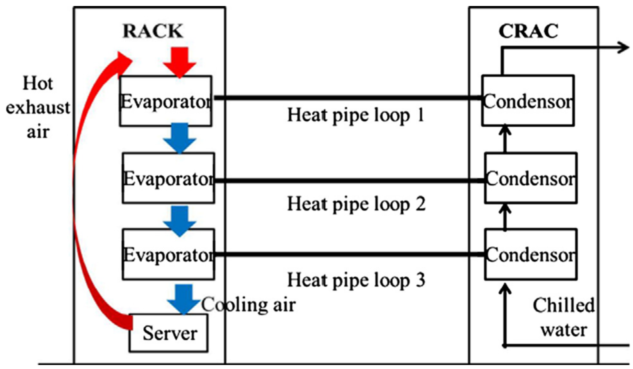

Fig. 14c. Air cooling solution with multi-stage heat pipe loop.

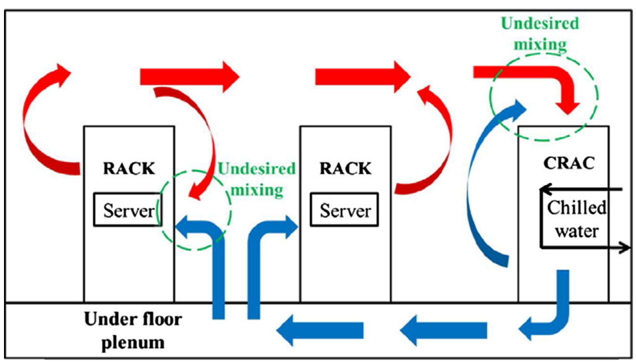

Fig. 14d. Air cooling solution with undesired mixings.

heat exchanging with a serially connected multi-stage heat pipe loop inside the rack. The heat is transferred from air side to the chilled water step-by-step, through each corresponding stage of heat pipe loop with individual temperature level, and finally transported to CRAC units.

Compared with liquid/ideal air cooling method, which introduce water terminals very close to servers, the heat pipe solution earns better security performance by using R134a as the cooling media, which turns into gas in case of local leakage, with much lower threat to servers than water drop. In addition, by maintaining the heat pipe temperature above the air dew point temperature in data center room, condensation of moisture can be avoided.

To further improve the thermal performance of the multi-stage heat pipe, a larger temperature range of both air circle and water loop is necessary [43], which can be realized by reducing the air and water mass flowrate. For such configuration of multi-stage heat pipe loop, larger temperature range of the two side fluids, and more stages of heat pipe loop brings in higher heat transfer efficiency [43]. As a consequence, a multi cold source with individual temperature level is allowed for each step of heat exchanging. Therefore, a better energy performance can be expected through a flexible combination of different cold sources with individual quality and temperature.

The entransy dissipation analysis on heat exchange, transport and removal for the four cooling solutions is illustrated by the *T-Q* chart in Fig. 15. For each cooling solution, the entransy dissipation is calculated from the heat source (CPU) to the cold source (CRAC unit). The horizontal solid line represents the uniform temperature which remains unchanged during heat transfer or exchange process (e.g., phase changing process), while the inclined solid line stands for a linear temperature variation with heat transfer or exchange (e.g., heating/cooling process of the single phase fluid). The two ends of the solid line stand for the temperature of intake/exhaust fluid (e.g., supply/return air of CRAC units, intake/exhaust air of servers, input/outflow chilled water of heat exchangers).

The entransy dissipation of CPU heat exchange with liquid/air is represented by the yellow region, which is enclosed by the horizontal solid line of CPU temperature and the inclined solid line of liquid/air temperature. The entransy dissipation of air mixing is represented by the deep green region, which is enclosed by the temperature solid line of air with rack and the temperature solid line of air with CRAC unit. The entransy dissipation of air to chilled water heat transfer is represented by the region enclosed by the solid line of air temperature and the solid line of chilled water temperature. The entransy dissipation of air to multi-stage heat pipe loop (three stage as exampled) heat transfer is represented by the trapezoid region, enclosed by the solid line of air temperature and the solid line of each stage heat pipe loop temperature. The entransy dissipation of chilled water to CRAC unit heat removal is represented by the region enclosed by the inclined solid line of

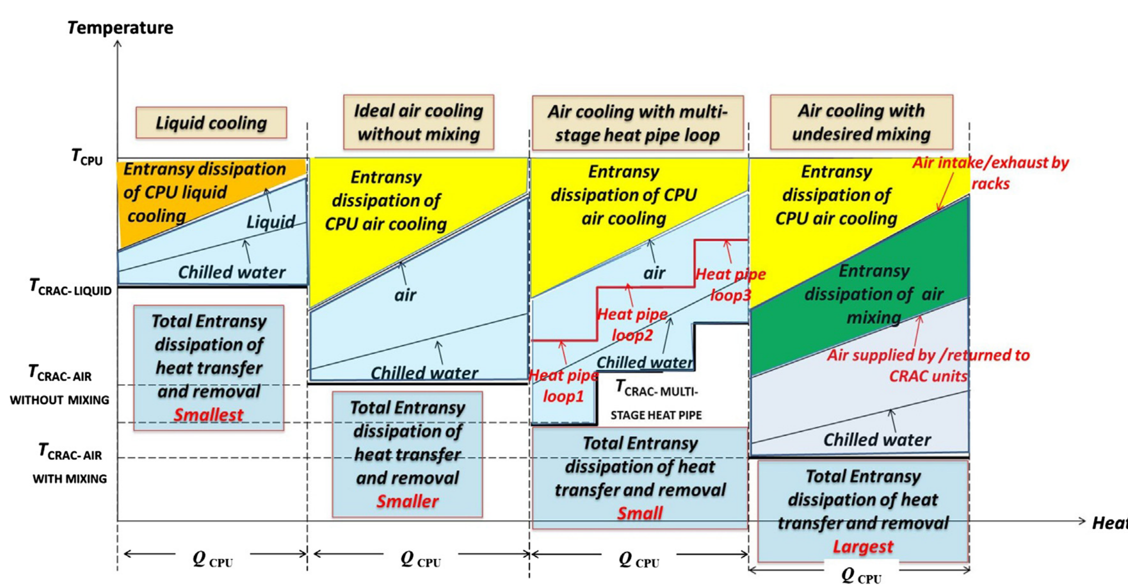

Fig. 15. T-Q chart for entransy dissipation analysis of the four cooling solutions.

chilled water temperature and the horizontal solid line of CRAC evaporator temperature.

The total entransy dissipation of heat transfer and removal is represented by the light blue region, which is enclosed by the inclined solid line of liquid/air temperature and the horizontal solid line of CRAC evaporator temperature. The total entransy dissipation of heat transfer and removal not only describes the heat transfer ability lost during heat transport process, it determines the temperature level of cold source and the availability of free cooling potential. Therefore, the area of such light blue regions offers quantitative evaluation and comparison for the energy performance of the four cooling solutions.

The slope of each inclined solid line represents the mass flowrate for each fluid, the more inclined of the solid line means the smaller mass flowrate of the fluid.

Tables 2 and 3 compute and list the temperature distribution and entransy dissipation for each heat transfer process for the four cooling solutions, respectively. To perform a fair analysis with comparable boundary conditions, the heat production, CPU temperature, and CRAC units remain the same for the four cooling solutions.

The entransy analysis tells that, due to the much higher heat transfer coefficient and no air mixing, the liquid cooling solution earns the best thermal performance with the smallest total entransy dissipation of 285 kW K, along with the highest cold source (CRAC evaporator) temperature of 291 K. As for the three air cooling solutions, due to the much lower heat transfer coefficient, most entransy (82–90%) is dissipated by the air involved heat transfer processes, resulting in a much higher total entransy dissipation of 418.13–540 kW K, and a much lower cold source (CRAC evaporator) temperature of 274–280 K, respectively. Meanwhile, compared with ideal air cooling, undesired air mixing consumes considerable heat transfer potential loss (18%), and contributes significantly to the decrease of energy performance (with the CRAC temperature reduced from 280 K to 274 K). The impact of undesired air mixing on energy performance is eventually paid by the 6 K reduce of CRAC temperature, or free cooling potential.

Table 4
Temperature distribution of two-stage and three-stage heat pipe loop.

Cooling solution	Two-stage heat pipe loop configuration	Three-stage heat pipe loop configuration
Heat transferred from servers, kW	15	15
Temperature of server intake/exhaust air, K	292/300	292/300
Temperature of each stage heat pipe loop, K	283.7/291.6	285/289/293
Temperature of input/output chilled water, K	281.5/289.5	281/289
Individual temperature of cold source corresponding to each stage of heat pipe loop, K	279.5/284.2	278/282/285
Cooling load distribution for each stage of heat pipe loop, %	35/65	28/36/36
Averaged cold source temperature, K	282.56	281.96

Table 5
Entransy dissipation comparison of two-stage and three-stage heat pipe loop.

Cooling solution	Two-stage heat pipe loop configuration	Three-stage heat pipe loop configuration
Entransy dissipated by heat transfer from rack side air to multi-stage heat pipe loops, kW K	107.5	97.5
Entransy dissipated by heat transfer from multi-stage heat pipe loops to chilled water, kW K	50	67.5
Entransy dissipated by heat transfer from chilled water to multi cold sources, kW K	44.2	43.13
Total entransy dissipation, kW K	201.7	208.13

Table 2
Temperature distribution of the four cooling solutions of data centers.

Cooling solution	Liquid cooling	Ideal air cooling	Air cooling with multi-stage heat pipe loop	Air cooling with undesired mixing
Heat removed from servers in a rack, kW	15	15	15	15
Server CPU temperature, K	310	310	310	310
Intake/exhaust liquid/air temperature of racks, K	300/306 (Liquid)	292/300 (Air)	292/300 (Air)	292/300 (Air)
Temperature of each stage heat pipe loop, K	–	–	285/289/293	–
Supply/return air temperature of CRAC unit, K	–	–	–	286/293
Chilled water input/output temperature, K	294/299	283/288	281/289	277/282
CRAC temperature, K	291	280	278/282/285	274

Table 3
Entransy dissipation analysis of the four cooling solutions of data centers.

Cooling solution	Liquid cooling	Ideal air cooling	Air cooling with multi-stage heat pipe loop	Air cooling with undesired mixing
Entransy dissipated by CPU heat exchanging, kW K	105	210	210	210
Entransy dissipated by liquid/air to chilled water heat exchanging, kW K	97.5 (liquid to chilled water)	157.5 (air to chilled water)	–	–
Entransy dissipated by rack side air to heat pipe loop heat exchanging, kW K	–	–	97.5	–
Entransy dissipated by undesired air mixing, kW K	–	–	–	97.5
Entransy dissipated by multi-stage heat pipe to chilled water heat exchanging, kW K	–	–	67.5	–
Entransy dissipated by CRAC side air to chilled water exchanging, kW K	–	–	–	150
Entransy dissipated by chilled water to CRAC exchanging, kW K	82.5	82.5	43.13	82.5
Entransy dissipation of heat transfer and removal (light blue region in Fig. 15), kW K	180	240	208.13	330
Total entransy dissipation, kW K	285	450	418.13	540

The entransy analysis also shows that, compared with the ideal air cooling scheme, the multi-stage heat pipe solution raises the temperature range of chilled water from 5 K to 8 K, to earn approximately the same entransy dissipation for the heat transfer between rack side air and chilled water (165 kW K v.s. 157.5 kW K), but with higher security performance than water terminals. Moreover, considering multi cold source with individual temperature (278/282/285 K), with the reasonable adjustment and assignment of cooling load to each cold source, the multi-stage heat pipe solution still owns the possibility to earn a better energy performance than the ideal air cooling solution (with cold source temperature of 280 K).

When compared with the air cooling scheme with undesired mixing, the multi-stage heat pipe solution earns a perfect victory with a higher cold source temperature (278/282/285 K v.s. 274 K), and a much smaller entransy dissipation for heat transfer and removal (the area of the light blue region in Fig. 15, 208.13 kW K v.s. 330 kW K).

To sum up, the entransy analysis on different cooling solutions of data centers clearly tells that, to effectively eliminate the undesired air mixing and improve the energy performance of data center thermal management, both the server-level liquid cooling solution and rack-level air cooling solution with multi-stage heat pipe loop seem possible. Considering the security performance, as well as the

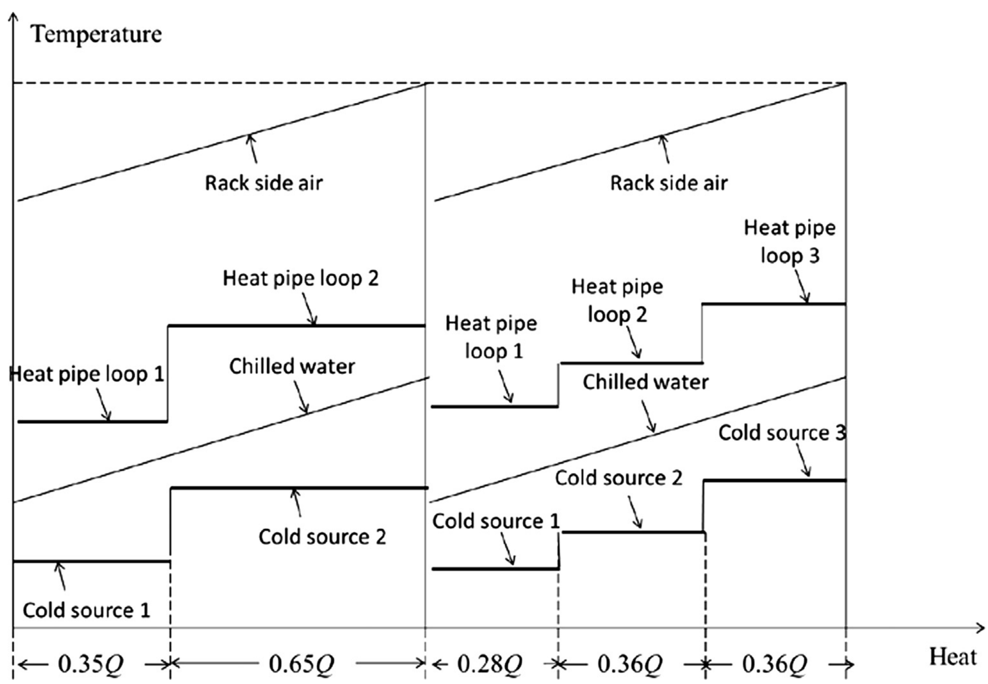

Fig. 16. Entransy dissipation analysis of two-stage and three-stage heat pipe loop in T-Q chart.

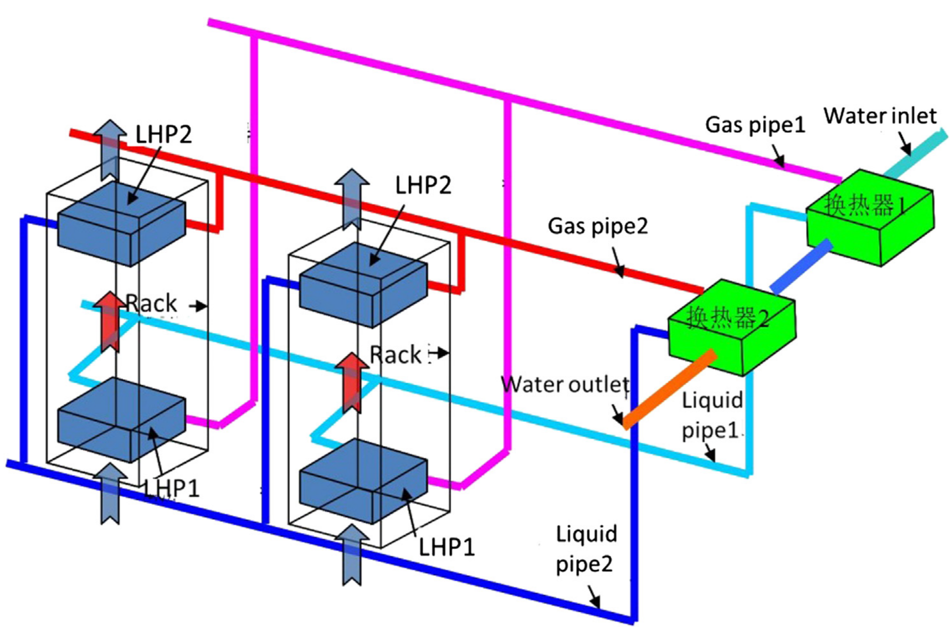

Fig. 17. Inner-cooled rack with a two-stage heat pipe loop.

diversity and availability of multi cold sources, the rack-level air cooling solution with multi heat pipe loop is proposed.

3.3.2. Combined rack-level air cooling solution

Based on the entransy dissipation analysis in Section 3.3.1, the rack-level air cooling solution combined with multi-stage heat pipe loop is proposed, as illustrated by Fig. 14(c). The former study [43] shows that, increasing the stages of heat pipe loops helps to improve thermal performance of such air-heat pipe-water heat transfer system. However, more heat pipe loops means the increase of initial investment and equipment size. To balance the thermal performance and cost, a deep analysis on entransy dissipation is performed, for the combined rack-level air cooling solution with two-stage and three-stage heat pipe loop configuration. To make the comparison fair and reasonable, the total heat exchanger area of the two-stage heat pipe loop equals to that of the three-stage heat pipe loop, with the same server heat (15 kW), CPU temperature (310 K) and server intake/exhaust air temperature (292/300 K). The cooling load taken by each stage of heat pipe loop can be adjusted to optimize the overall thermal performance.

The optimum cooling load assignment, temperature distribution and entransy dissipation for each heat pipe configuration is computed and listed in Tables 4 and 5, respectively.

The analysis above tells that, with the same total heat exchanging area and the optimized cooling load allocation, the overall thermal performance of the two heat pipe loop configurations remain the same level, in terms of cold source temperature and entransy dissipation distribution. To be specific, with the cooling load

Fig. 18. Photos of new combined rack-level air cooling equipments after retrofitting.

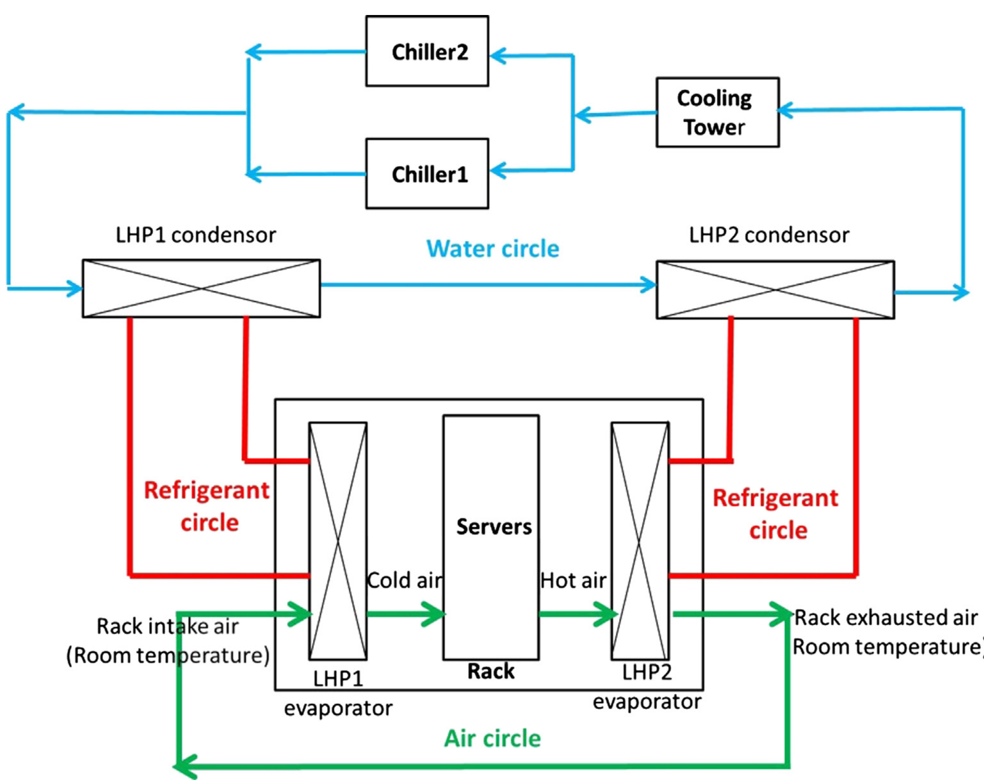

Fig. 19. Schematic diagram of parallel connected chillers.

distribution of 35%/65% for each stage of heat pipe loop, the optimum individual cold source temperature of the two-stage configuration is 279.5 K/284.2 K, almost the same with that of the three-stage configuration (278 K/282 K/285 K). To further compare the energy performance, the averaged temperature of individual cold sources weighted by cooling load allocation is calculated for each heat pipe configuration, which is also listed in Table 4. It can be seen that, the two-stage heat pipe configuration earns a little better energy performance with averaged cold source temperature 0.6 K higher than that of three-stage configuration (282.56 K v.s. 281.96 K). This conclusion can also be proved with the entransy analysis, the two-stage configuration outplayed the three-stage one with a smaller entransy dissipation (201.7 kW K v.s. 208.13 kW K).

Fig. 16 illustrates the temperature distribution and entransy dissipation of these two heat pipe configurations, in terms of *T-Q*

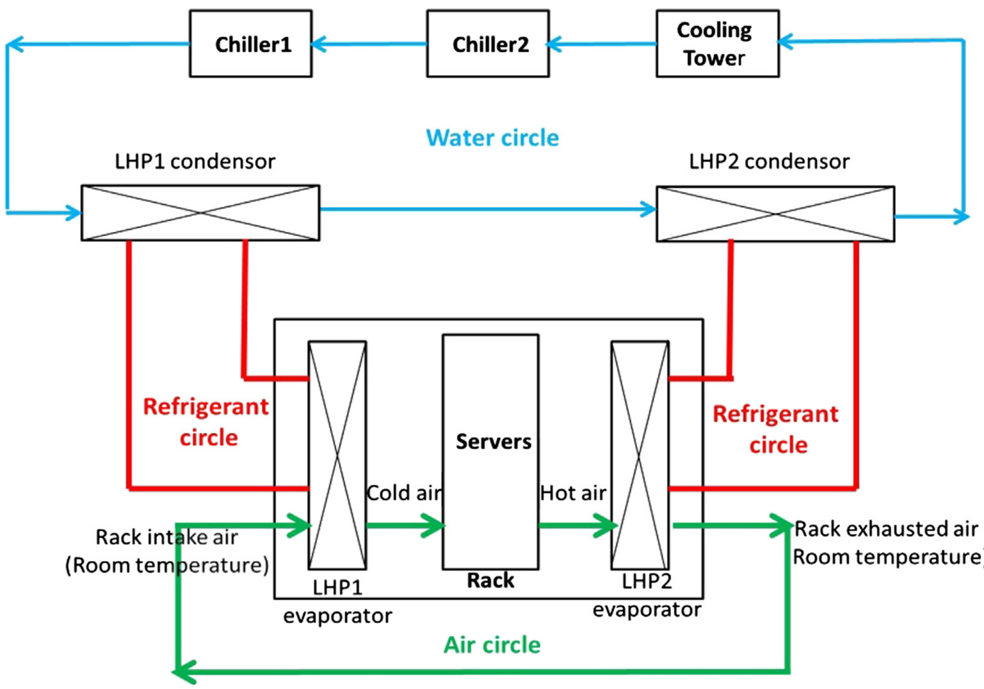

Fig. 20. Schematic diagram of serial connected chillers.

Table 6
Performance comparison of the two water-side cooling solutions.

Water loop	Chiller	Inlet/outlet water temp	Water flow rate	NTU	Cold source temp	Chiller energy cost	Entransy dissipation of water loop
Parallel	Chiller1	10 °C/14 °C	3.75 kW/K	1.5	8.85 °C	4.15 kW	300 kW K
	Chiller2	10 °C/14 °C	3.75 kW/K	1.5	8.85 °C	4.15 kW	
Serial	Chiller1	14 °C/18 °C	3.75 kW/K	1.5	12.85 °C	3.56 kW	240 kW K
	Chiller2	10 °C/14 °C	3.75 kW/K	1.5	8.85 °C	4.15 kW	

(a) Closed cooling tower (b) Two serial connected chillers

Fig. 21. Combined water loop after retrofitting.

chart, which gives intuitional and comparable views of entransy dissipation analysis for each heat exchanging and heat transfer process.

Based on the entransy analysis above, to balance the investment and performance, the configuration of two-stage heat pipe loop is proposed as the final scheme of rack level air-cooling solution, illustrated by Fig. 17. The inlet air with the same temperature as data center room is cooled down by the first stage of heat pipe loop (with lower temperature) at the bottom of racks, to the required inhale temperature of servers. Then the hot exhaust air from servers is sent to the second stage of heat pipe loop (with higher temperature) at the top of racks, cooled down to the room temperature and released into data center room again. The entire heat exchange and transport process is sealed inside the rack, maintaining no temperature difference between the rack side intake/exhaust air and ambient room air. Therefore the undesired air mixings can be avoided.

After retrofitting, the photos of new combined air cooling racks with two-stage heat pipe loop is shown by Fig. 18.

3.3.3. Combined water loop solution with larger temperature range

To fit the requirement of larger temperature range with smaller mass flowrate, individual cold sources with different quality and temperature, adjustable cooling load distribution, corresponding to the rack-side configuration of two-stage heat pipe loop, a combined water loop solution with parallel/serial connected chillers is proposed for the water-side configuration, illustrated by Figs. 19 and 20, respectively. The detailed performance of these two water-side configurations is evaluated and compared by entransy dissipation analysis, listed in Table 6.

The entransy analysis tells that, compared with the scheme of parallel connected chillers, chiller configuration with serial connection earns a better entransy performance, with the total entransy dissipation decreased from 300 kW K to 240 kW K, indicating a free cooling potential (e.g., output water from cooling towers) increase of 4 K (with heat removal of 15 kW).

Based on entransy analysis above, considering the initial investment and operating cost, the final scheme of water-side configuration is designed as two chillers serial connected with a closed cooling tower, illustrated by Fig. 21. The operating mode of the combined water loop depends on the output water from the closed cooling tower. With low enough output water temperature, all cooling load is took by the closed cooling tower with no chiller working, which is called full free cooling mode. When the output water temperature gradually rises, chillers start one by one to undertake partial cooling load, which is called co-working mode. To maximize the energy performance, cooling load is dynamically allocated among the cooling tower and two chillers, according to the outdoor air temperature change.

3.4. Performance testing after retrofitting

Fig. 22 shows the real time air temperature inside a LHP rack after retrofitting. It can be seen that the temperature curve of LHP1 inlet air coincides with that of LHP2 exhausted air, indicating identical rack intake and exhaust air temperature of 23–25 °C (average indoor temperature). The average intake air temperature of IT equipment (LHP1 exhausted air temperature) varies from 17.5 °C to 21 °C, satisfied with the guidelines of data processing environment recommended by TC 9.9 ASHERA.

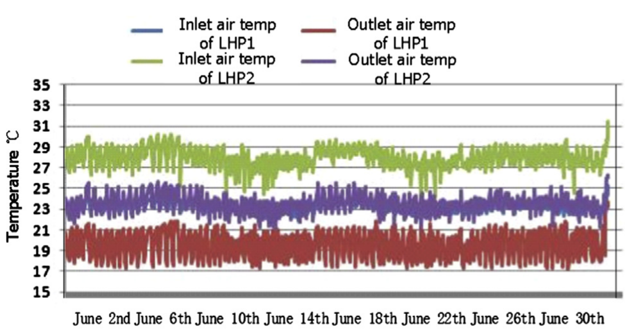

Fig. 22. Real time air temp inside a typical LHP rack after retrofitting.

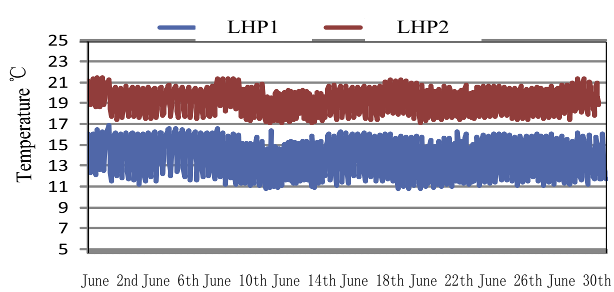

Fig. 24. Real time chilled water temp of LHP1 and LHP2 after retrofitting.

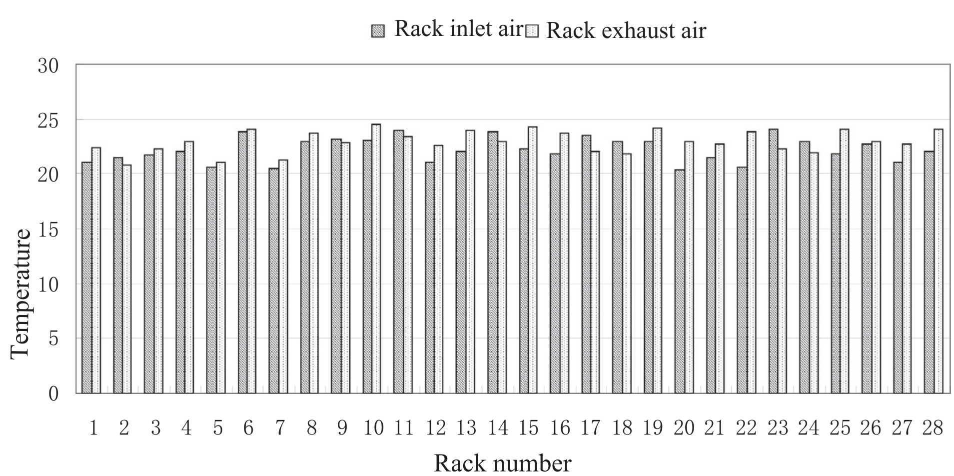

Fig. 23. Tested inlet and outlet air temp of all racks after retrofitting.

Table 7
Annual cooling performance of former CRAC system before retrofitting.

Time	CRAC power kW	Fan power kW	Server power kW	*EER* –	Indoor air temp °C	Evaporator temp °C	Supply/Return air temp °C	Rack inlet/outlet air temp °C	Outdoor dry/wet bulb temp °C
January 2nd	16.8	4.5	58	2.7	23.5	8.7	14/24	24/33	6/0.2
May 7th	18	4.2	56	2.5	24.6	8.5	15/25	24/33	20/10
August 10th	21	4.6	58	2.3	25	8.2	14/25	25/34	29/21

Table 8
Annual cooling performance of new combined cooling system after retrofitting.

Time	Cooling tower power kW	Chiller 1 power kW	Chiller 2 power kW	Pump power kW	Rack fan power kW	Server power kW	*EER* –	Indoor air temp °C	Supply/return water temp °C	Rack inlet/outlet air temp °C
January 2nd	2.2	0	0	2	2.9	58	8.2	23.5	9.5/18	23.8/24.2
May 7th	2.2	7.6	0	2	3.1	58	4.0	24.6	13.5/21.5	24.9/25.3
August 10th	0	6.4	6.8	2	3.1	59	3.2	23	9.2/19	23.2/23.8

Fig. 23 gives the intake and exhausted air temperature of all racks after retrofitting. The largest temperature difference between inlet and outlet air is less than 2.5 °C, indicating a great improvement of indoor environment compared with that before retrofitting.

The water loop temperature for corresponding LHP is shown in Fig. 24. Chilled water with higher temperature (18–21 °C) in LHP2 earns more energy benefits than that with lower temperature (12–16 °C) in LHP1 in chiller-working mode, and is more feasible to free cooling utilization.

Annual energy performance of former CRAC scheme and new combined cooling solution is tested and compared by Tables 7 and 8. The tests are performed with same climate conditions and IT payload distribution. The energy efficiency ratio (*EER*) is defined as the ratio of total cooling load to the total cooling power consumption, indicating the overall energy efficiency of cooling systems.

It can be seen from Tables 7 and 8 that, before retrofitting, the average temperature of rack exhausted air is about 9 °C higher than room temperature, and after retrofitting, the two temperature is almost the same, indicating a satisfied effect of eliminating undesired air mixing. Without temperature penalty paid for the air-mixing, the testing results also witness a temperature rise for cold source (outdoor air wet-bulb temperature) from 0.2 °C/10 °C to 9.5 °C/13.5°Cin January/May. With such additional free cooling potentials earned, a better energy performance can be expected.

By the co-operation of free cooling combined with multi-stage heat pipe loops, the annual energy efficiency ratio (*EER*) of cooling system increases from 2.6 to 4.8 after retrofitting, which means almost a double time of overall energy performance for the new combined distributed cooling solution than former CRAC system.

To sum up, the testing data above tells that, with the elimination of air-mixing, and full utilization of outdoor free cooling potential, both thermal and energy performance of data centers can be effectively improved. The inner-cooled rack with two-stage heat pipe loop creates a more uniform indoor thermal environment by dynamic allocation of cold air to avoid cooling-starving racks and undesired air-mixing. The co-operation mode of closed cooling tower with serially connected multi-chillers provides a maximum energy efficient through dynamic fit to the variation of outdoor climate and indoor payload.

4. Conclusion

The heat transfer process in data centers turns out to be better analyzed and optimized using entransy theory. Based on entransy dissipation theory, a multi-level entransy model for data center thermal management is built and verified with a CRAC retrofitting case. For the quantitative effect of undesired air mixing on thermal performance of data center cooling, which used to be very difficult with traditional thermal methods, entransy dissipation model gives quantitative analysis in terms of temperature penalty and free cooling potential loss, with enough accuracy. Through the case study of CRAC retrofitting work for an operating data center in Beijing, the entransy method is testified and proved to offer a new mathematical solution to the analysis and optimization of thermal management of data centers. A feasible technical route for key issues of local over-heating and huge energy cost in high heat density data centers may be found from this entransy based thermal method and combined cooling solution.

The major conclusions of this work have been summarized as follows:

1. Temperature rise must be paid as a penalty for air mixings with temperature differences among data center space, as the major reason for hot spot and cooling-starving racks.
2. Smaller entransy dissipation is found in multi-stage heat pipe loops combined inside racks than single-stage configuration.
3. The inner cooled racks with two-stage heat pipe loops enables to eliminate air mixings with no temperature differences, by maintaining the exhausted air with the same temperature as room environment.
4. Smaller entransy dissipation is found with serial chillers layout than that in parallel, with the same outdoor climate and indoor payload.
5. A closed cooling tower combined with serially connected chillers maximizes both the outdoor free cooling potential and energy performance, by dynamic adjustment and re-designation of the cooling load in co-operation.

Conflict of interest

There are no conflicts of interest for all authors of this paper.

References

[1] Y. Fulpagare, A. Bhargav, Advances in data center thermal management, Renew. Sustain. Energy Rev. 43 (2015) 981–996.
[2] H. Zhang, S. Shao, H. Xu, H. Zou, C. Tian, Free cooling of data centers: a review, Renew. Sustain. Energy Rev. 35 (2014) 171–182.
[3] K. Ebrahimi, G.F. Jones, A.S. Fleischer, A review of data center cooling technology, operating conditions and the corresponding low-grade waste heat recovery opportunities, Renew. Sustain. Energy Rev. 31 (2014) 622–638.

[4] S.V. Garimella, T. Persoons, J. Weibel, L.-T. Yeh, Technological drivers in data centers and telecom systems: multiscale thermal, electrical, and energy management, Appl. Energy 107 (2013) 66–80.
[5] S.-W. Ham, M.-H. Kim, B.-N. Choi, J.-W. Jeong, Simplified server model to simulate data center cooling energy consumption, Energy Build. 86 (2015) 328–339.
[6] H. Tian, Z. He, Z. Li, A combined cooling solution for high heat density data centers using multi-stage heat pipe loops, Energy Build. 94 (2015) 177–188.
[7] K.-P. Lee, H.-L. Chen, Analysis of energy saving potential of air-side free cooling for data centers in worldwide climate zones, Energy Build. 64 (2013) 103–112.
[8] J. Siriwardana, S. Jayasekara, S.K. Halgamuge, Potential of air-side economizers for data center cooling: a case study for key Australian cities, Appl. Energy 104 (2013) 207–219.
[9] T. Gao, M. David, J. Geer, R. Schmidt, B. Sammakia, Experimental and numerical dynamic investigation of an energy efficient liquid cooled chiller-less data center test facility, Energy Build. 91 (2015) 83–96.
[10] A. Carbó, E. Oró, J. Salom, M. Canuto, M. Macías, J. Guitart, Experimental and numerical analysis for potential heat reuse in liquid cooled data centres, Energy Convers. Manage. 112 (2016) 135–145.
[11] S.A. Nada, M.A. Rady, M. Elsharnoby, M.A. Said, Numerical investigation of cooling of electronic servers racks at different locations and spacing from the data center cooling unit, Int. J. Curr. Eng. Technol. 5 (5) (2015).
[12] V. Sorell, S. Escalante, J. Yang, Comparison of overhead and under floor air delivery systems in a data center environment using CFD modeling, ASHRAE Trans. 111 (2) (2005).
[13] S.T. Kadam, R. Kumar, Twenty first century cooling solution: micro-channel heat sinks, Int. J. Therm. Sci. 85 (2014) 73–92.
[14] S.A. Nada, M.A. Said, M.A. Rady, Numerical investigation and parametric study for thermal and energy management enhancements in data centers buildings, Appl. Therm. Eng. 98 (2016) 110–128.
[15] S.A. Nada, K.E. Elfeky, A.M.A. Attia, W.G. Alshaer, Thermal management of electronic servers under different power conditions, Int. J. Emerg. Trends Electr. Electron. 11 (4) (2015) 145–150.
[16] S.A. Nada, K.E. Elfeky, A.M.A. Attia, Experimental investigations of air conditioning solutions in high power density data centers using a scaled physical model, Int. J. Refrig. 63 (2016) 87–99.
[17] S.A. Nada, K.E. Elfeky, Experimental investigations of thermal managements solutions in data centers buildings for different arrangements of cold aisles containments, J. Build. Eng. 5 (2016) 41–49.
[18] S.A. Nada, A.M.A. Attia, K.E. Elfeky, Experimental study of solving thermal heterogeneity problem of data center servers, Appl. Therm. Eng. 109 (2016) 466–474.
[19] W. Abdelmaksoud, Experimental and Numerical Investigations of the Thermal Environment in Air-Cooled Data Centers (Ph.D. thesis), Department of Mechanical and Aerospace Engineering, Syracuse University, Syracuse, NY, 2012.
[20] J. Cho, J. Yang, W. Park, Evaluation of air distribution system's airflow performance for cooling energy savings in high-density data centers, Energy Build. 68 (2014) 270–279.
[21] J. Priyadumkol, C. Kittichaikarn, Application of the combined air-conditioning systems for energy conservation in data center, Energy Build. 68 (2014) 580–586.
[22] T. Lu, Remes M LüX, M. Viljanen, Investigation of air management and energy performance in a data center in Finland: case study, Energy Build. 43 (12) (2011) 3360–3372.
[23] J. Siriwardana, S.K. Halgamuge, T. Scherer, W. Schott, Minimizing the thermal impact of computing equipment upgrades in data centers, Energy Build. 50 (2012) 81–92.
[24] M. Lin, S. Shao, X. Zhang(Simon), J.W. VanGilder, V. Avelar, X. Hu, Strategies for data center temperature control during a cooling system outage, Energy Build. 73 (2014) 146–152.
[25] V.K. Arghode, P. Kumar, Y. Joshi, T.S. Weiss, Rack level modeling of air flow through perforated tile in a data center, J Electron Packag. 135 (3) (2013) 1–11.
[26] V. López, H.F. Hamann, Heat transfer modeling in data centers, Int J Heat Mass Transf. 54 (25–26) (2011) 5306–5318.
[27] R.J. McGlen, R. Jachuck, S. Lin, Integrated thermal management techniques for high power electronic devices, Appl. Therm. Eng. 24 (2004) 1143–1156.
[28] A. Almoli, A. Thompson, N. Kapur, J. Summers, H. Thompson, G. Hannah, Computational fluid dynamic investigation of liquid rack cooling in data centres, Appl Energy 89 (1) (2012) 150–155.
[29] S. Bhopte, D. Agonafer, R. Schmidt, B. Sammakia, Optimization of data center room layout to minimize rack inlet air temperature, J Electron Packag. 128 (4) (2006) 380.
[30] B. Fakhim, M. Behnia, S.W. Armfield, N. Srinarayana, Cooling solutions in an operational data centre: a case study, Appl Therm Eng. 31 (14–15) (2011) 2279–2291.
[31] Amip Jagat Shah, Exerg-Based Analysis and Optimization of Computer Thermal Management Systems, University of California Department of Mechanical Engineering, Berkeley, 2005.
[32] J. Rambo, Y. Joshi, Modeling of data center airflow and heat transfer: state of the art and future trends, Distrib. Parallel Datab. 21 (2) (2007) 193–225.
[33] Zhou Rongliang Bash, Wang Zhikui, et al., Data center cooling management and analysis – a model based approach, in: The 28th Annual IEEE Semiconductor Thermal Measurement and Management Symposium, SEMI-THERM 2012, 2012, pp. 98–103.
[34] Z.Y. Guo, X.G. Cheng, Z.Z. Xia, Least dissipation principle of heat transport potential capacity and its application in heat conduction optimization, Chin. Bull. 4 (48) (2003) 406–410.
[35] Z.Y. Guo, H.Y. Zhu, X.G. Liang, Entransy: a physical quantity describing heat transfer ability, Int. J. Heat Mass Transfer 50 (2007) 2545–2556.
[36] Z.Y. Guo, New physical quantities in heat, J. Eng. Thermophys. 29 (2008) 112–114.
[37] M. Xu, The thermodynamic basis of entransy and entransy dissipation, Energy 36 (2011) 4272–4277.
[38] X.G. Cheng, Z.X. Li, Z.Y. Guo, Variational principles in heat conduct, J. Eng. Thermophys. 25 (2004) 457–459.
[39] X.T. Cheng, X.G. Liang, Z.Y. Guo, Principle of entransy dissipation for heat transfer in an isolated system, Sci. Bull. 56 (2011) 222–230.
[40] W. Liu, Z. Liu, H. Jia, et al., Entransy expression of the second law of thermo - dynamics and its application to optimization in heat transfer process, Int. J. Heat Transfer 54 (2011) 3049–3059.
[41] G.J. Hu, Z.Y. Guo, The efficiency of heat transfer process, J. Eng. Thermophys. 32 (2011) 1005–1008.
[42] Q. Chen, J. Wu, M. Wang, N. Pan, Z.Y. Guo, A comparison of optimization theories for energy conservation in heat exchanger groups, Chin. Sci. Bull. 56 (4–5) (2011) 449–454.
[43] Z. Li, H. Tian, H.Q. Zhang, et al., Performance optimization of separate type heat pipe heat exchanger in plant room with high density of sensible heat load, HV&AC 3 (41) (2011) 38–43.